

Supplementary Material: “Climate change decouples drought from early wine grape harvests in Western Europe”

Benjamin I Cook^{1,2} & Elizabeth M Wolkovich^{3,4}

April 1, 2015

Individual Site Analyses.

Temperature versus Moisture Comparisons.

Table 1: Regional GHD series from DAUX used in construction of the GHD-Core composite series. Included are the codes for each site, their geographic locations (units of decimal degrees), and their mean harvest dates for various intervals.

GHD Series	Site Code	Lat	Lon	1600-1900	1600-1980	1901-1950	1951-1980	1981-2007
Alsace	Als	48.17	7.28	282.81	281.87	272.12	287.16	277.70
Bordeaux	Bor	45.18	-0.75	269.01	268.22	263.85	270.41	259.75
Burgundy	Bur	47.32	5.04	269.92	270.07	269.44	272.58	262.15
Champagne 1	Chal	47.98	4.28	266.88	267.52	267.01	270.02	264.92
Low Loire Valley	LLV	47.15	0.22	286.12	284.61	282.69	282.56	275.33
Southern Rhone Valley	SRv	43.98	5.05	269.20	269.10	268.84	268.46	257.87
Switzerland (Lake Geneva)	Swi	46.57	6.52	286.39	283.87	273.86	275.22	263.00

Table 2: For various intervals , the fraction of years for each regional GHD series for which observations are available.

	1354-2007	1600-1900	1600-2007	1800-2007	1900-2007
Als	0.400612	0.578073	0.642157	0.836538	0.824074
Bor	0.500000	0.647841	0.737745	0.995192	0.990741
Bur	0.925076	0.996678	0.990196	0.985577	0.972222
Cha2	0.279817	0.259136	0.448529	0.879808	0.981481
LLV	0.310398	0.332226	0.497549	0.975962	0.962963
SRv	0.689602	0.970100	0.950980	0.942308	0.898148
Swi	0.749235	1.000000	1.000000	1.000000	1.000000

Table 3: Spearman's rank correlations (1600-2007) between each regional GHD series used in construction of the GHD-Core index.

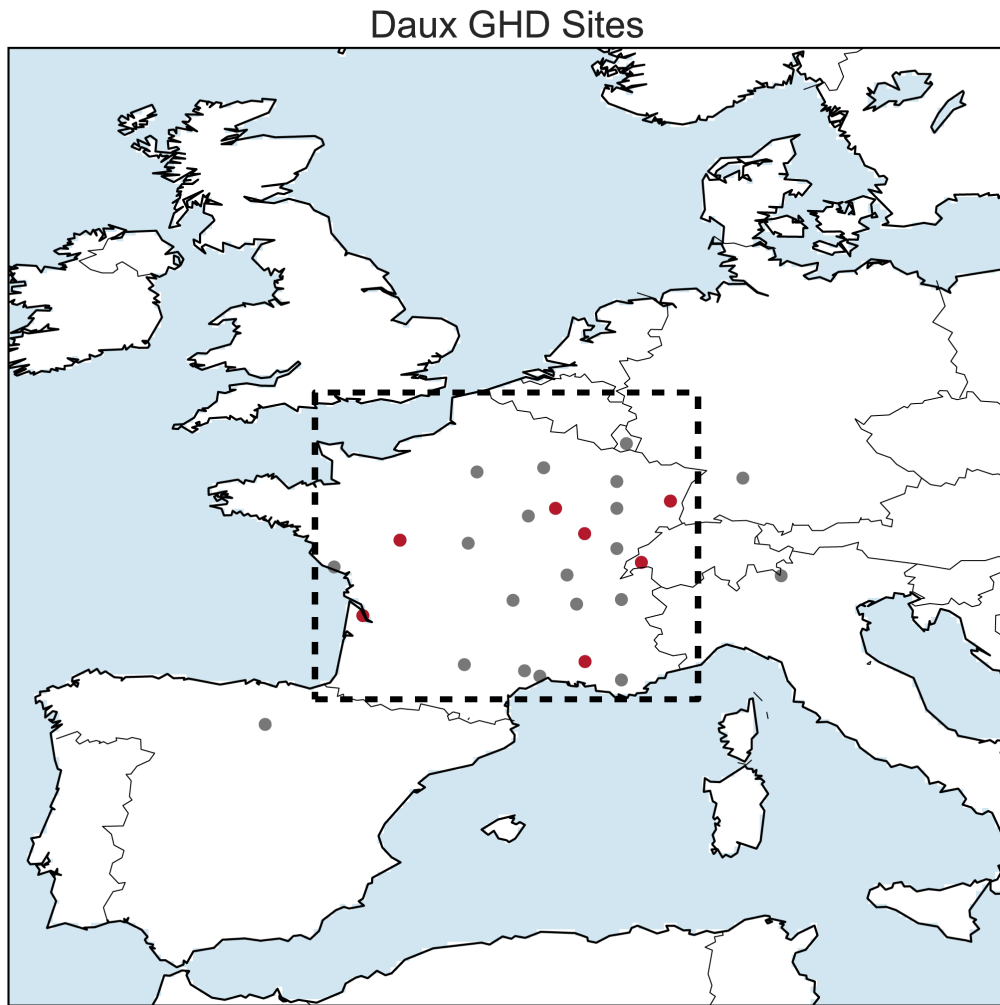
	Als	Bor	Bur	Cha1	LLV	SRv	Swi
Als	1	0.601045	0.573844	0.632206	0.502502	0.413751	0.604378
Bor	0.601045	1	0.622279	0.675208	0.712442	0.321238	0.547885
Bur	0.573844	0.622279	1	0.798581	0.775801	0.542594	0.582605
Cha1	0.632206	0.675208	0.798581	1	0.709044	0.346222	0.569444
LLV	0.502502	0.712442	0.775801	0.709044	1	0.456008	0.696642
SRv	0.413751	0.321238	0.542594	0.346222	0.456008	1	0.525608
Swi	0.604378	0.547885	0.582605	0.569444	0.696642	0.525608	1

Table 4: Anomalies in GHD, calculated relative to the baseline mean baseline calculated for 1600-1900. Also included are results for the GHD-Core index and GHD-All, composed from all 27 regional GHD series in DAUX. GHD-Core and GHD-All represent the composite average AFTER the anomalies of the individual regional GHD series.

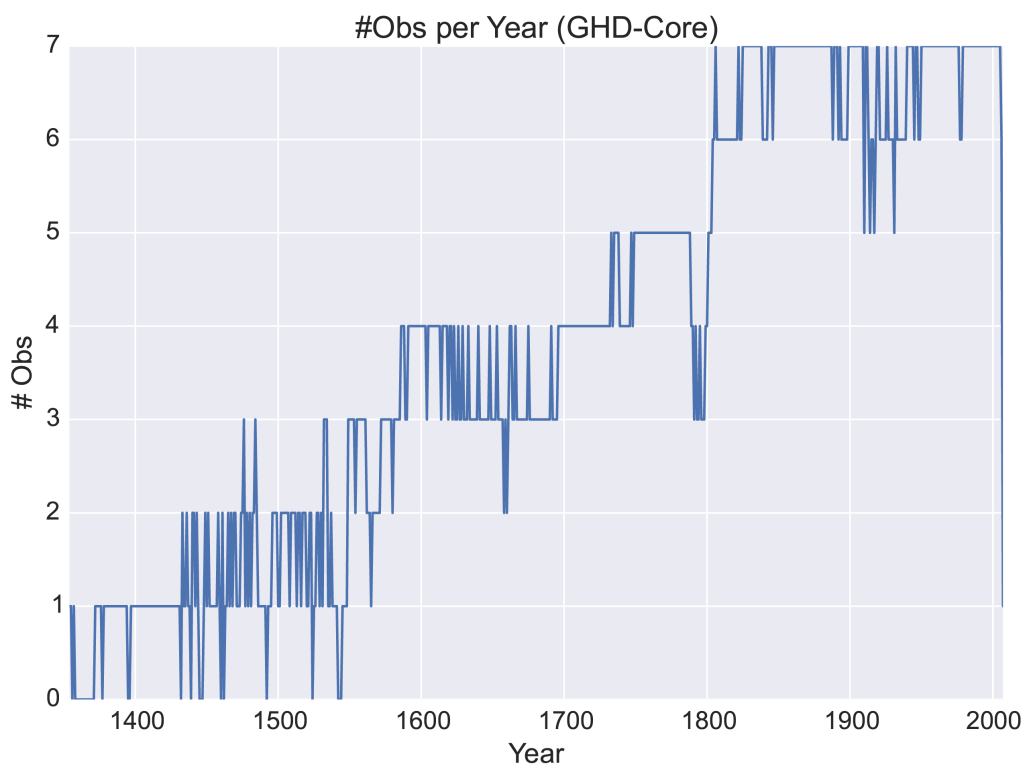
	1600-1900	1600-1980	1901-1950	1951-1980	1981-2007
Als	0	-0.94	-10.69	4.35	-5.11
Bor	0	-0.79	-5.16	1.40	-9.26
Bur	0	0.15	-0.48	2.66	-7.78
Cha1	0	0.64	0.13	3.14	-1.96
LLV	0	-1.51	-3.42	-3.56	-10.79
SRv	0	-0.10	-0.36	-0.74	-11.33
Swi	0	-2.52	12.53	11.17	23.39
GHD-Core	-0.35	-0.91	-4.49	-0.47	-10.62
GHD-All	-0.25	-0.85	-5.13	0.36	-8.91

Table 5: As Table 4, but for inter-annual standard deviation.

	1600-1900	1600-1980	1901-1950	1951-1980	1981-2007
Als	8.74	9.56	9.12	7.09	8.74
Bor	9.51	9.00	6.27	7.00	9.56
Bur	9.61	9.19	6.55	8.11	7.97
Chal	8.81	8.88	7.85	10.12	8.64
LLV	10.29	9.21	6.56	8.01	7.41
SRv	8.68	8.46	8.62	5.55	5.93
Swi	10.09	10.71	7.19	6.68	8.11
GHD-Core	7.80	7.57	5.50	6.61	7.92
GHD-All	7.03	7.02	5.55	6.55	6.75

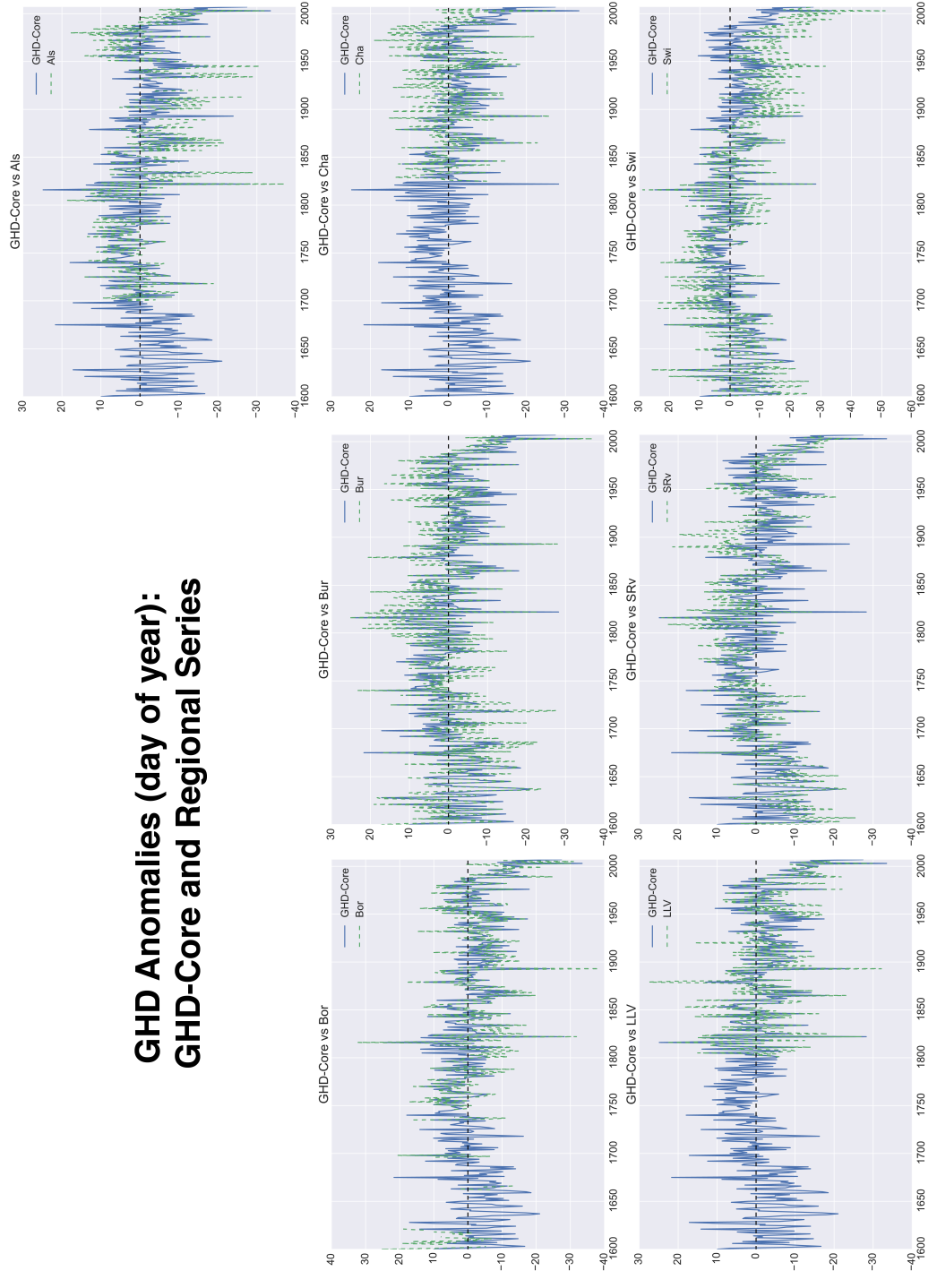


Supplementary Figure 1: Geographic locations for all 27 regional GHD time series in DAUX. Highlighted in red are the sites that comprise the GHD-Core index: Alsace (Als), Bordeaux (Bor), Burgundy (Bur), Champagne 1 (Cha1), the Lower Loire Valley (LLV), the Southern Rhone Valley (SRv), and Switzerland at Lake Geneva (Swi). The dashed black box indicates the GHD-Core region (2°W – 8°E , 43°N – 51°N) over which climate anomalies from the CRU instrumental climate datasets and the three reconstructions were averaged for the various regression analyses.

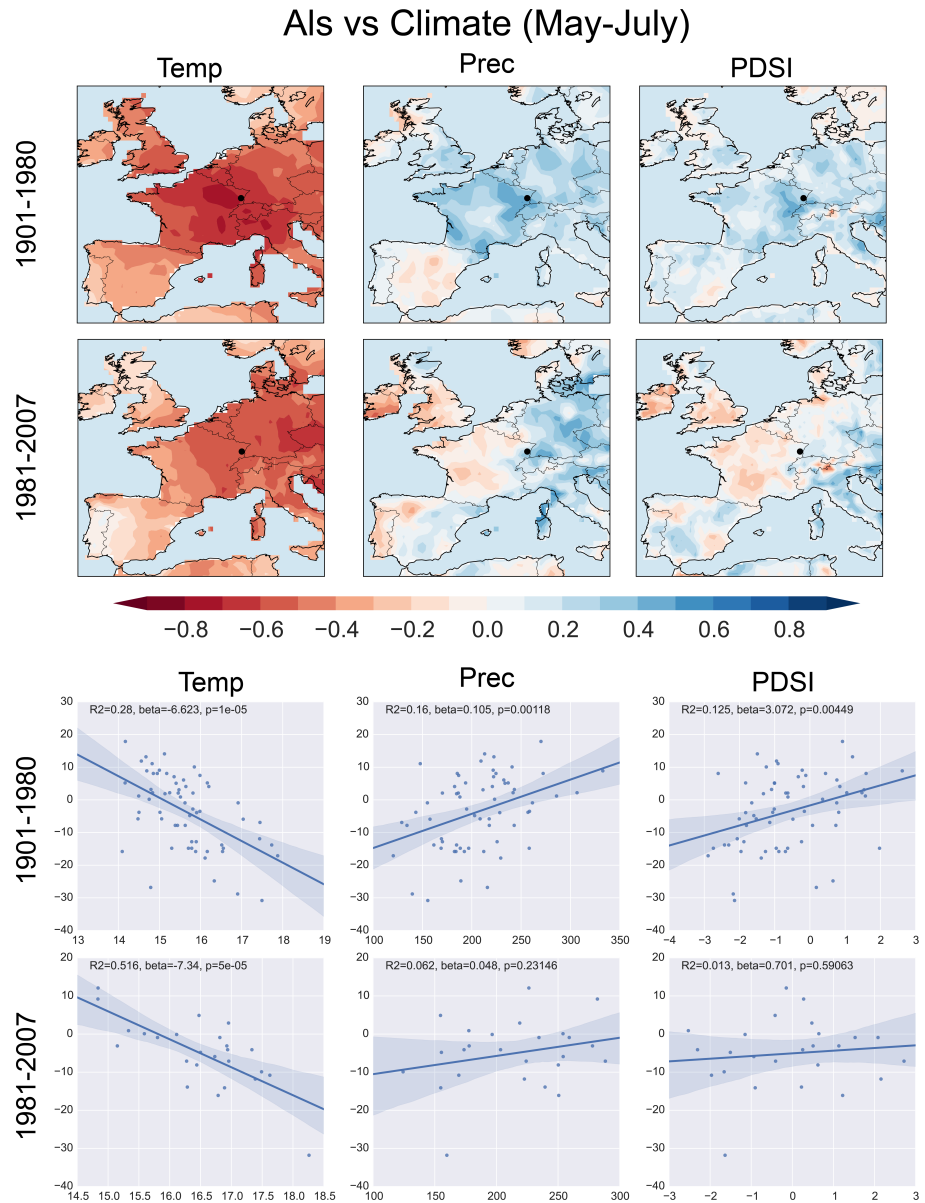


Supplementary Figure 2: Number of observations (i.e., regional GHD series) represented in each year of the GHD-Core index.

GHD Anomalies (day of year): GHD-Core and Regional Series

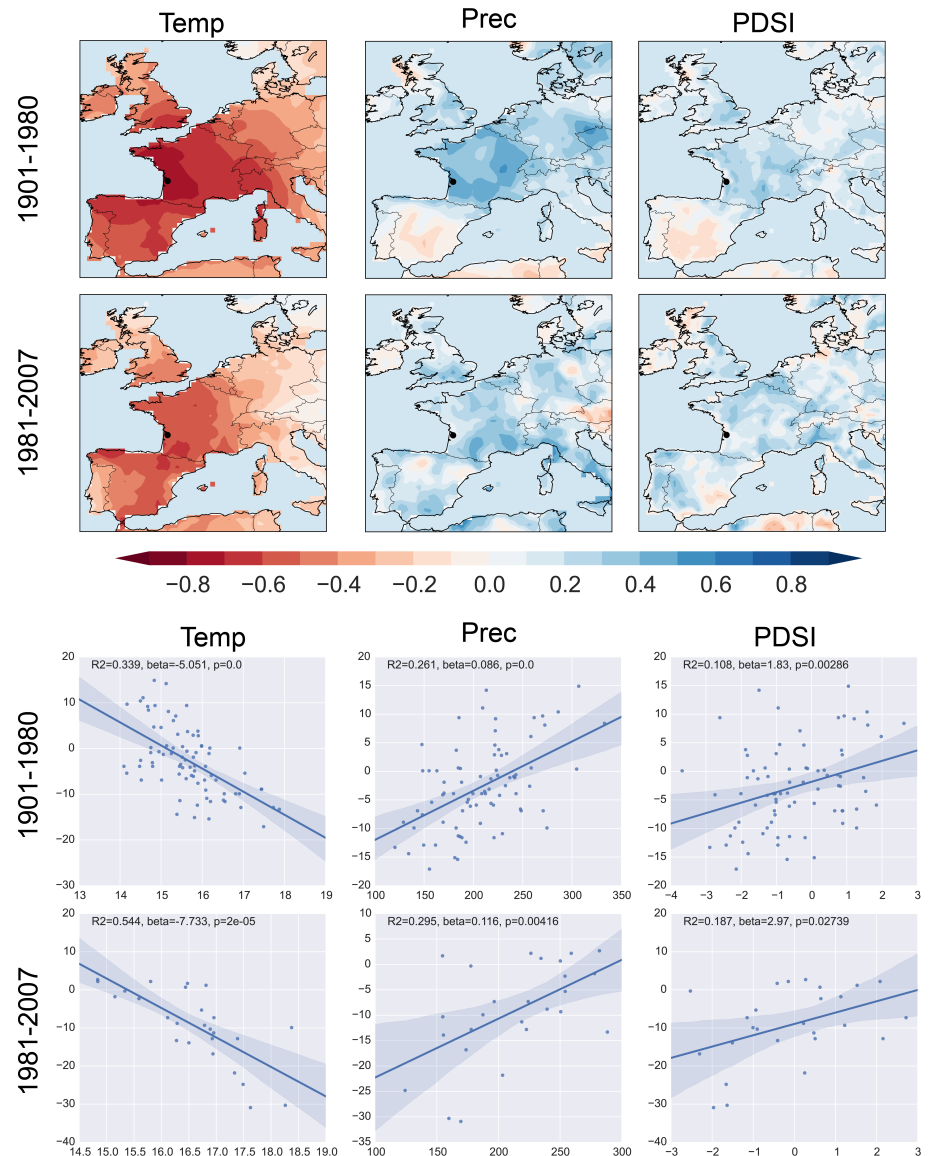


Supplementary Figure 3: Time series (1600–2007) of GHD-Core (blue solid line) and each individual regional GHD series (green dashed lines).

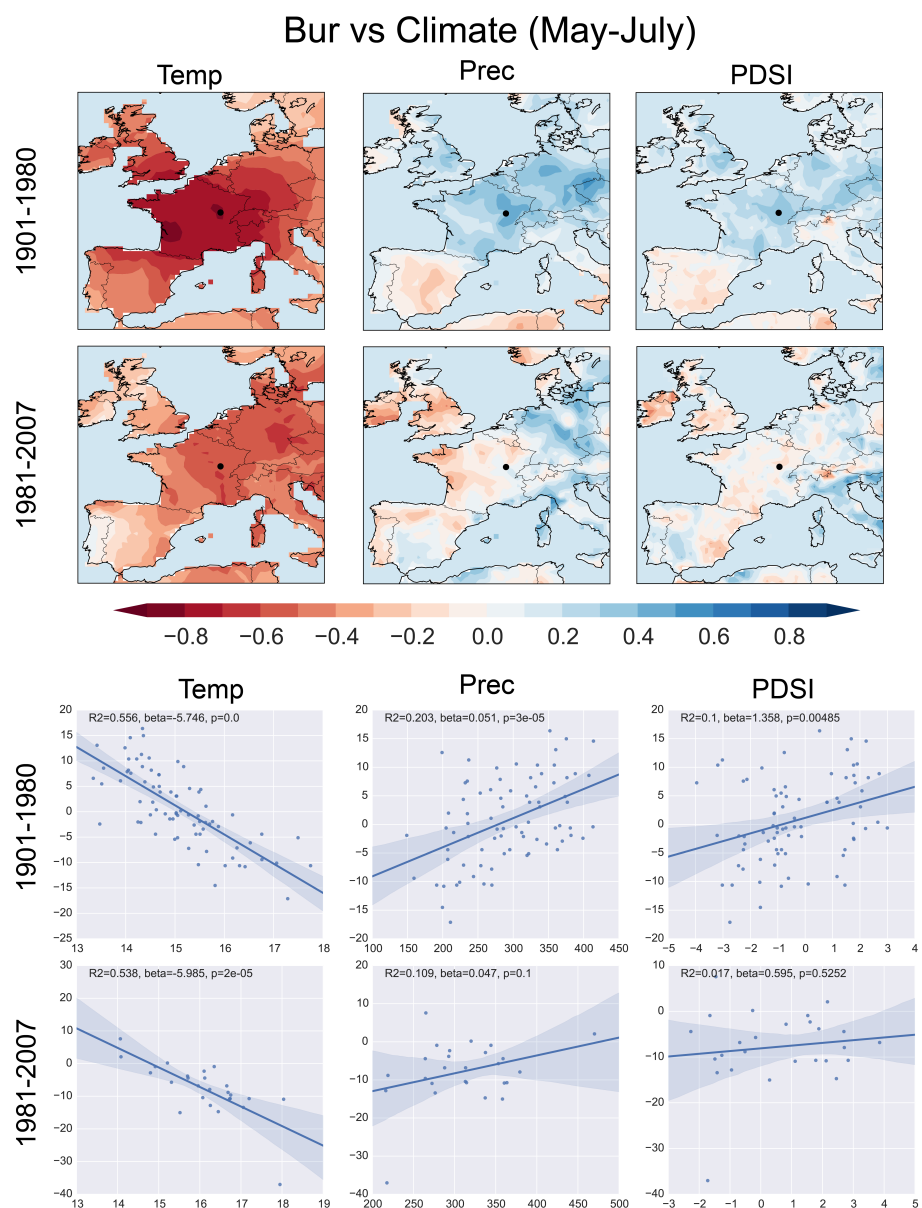


Supplementary Figure 4: Comparisons between the GHD series from ALS and May-June-July temperature, precipitation, and PDSI from the CRU 3.21 climate grids. Top panels: point-by-point correlations for 1901–1980 and 1981–2007 (location of ALS is shown by the black dot). Bottom panels: linear regression plots for the same intervals against CRU climate data averaged within one degree of the site location.

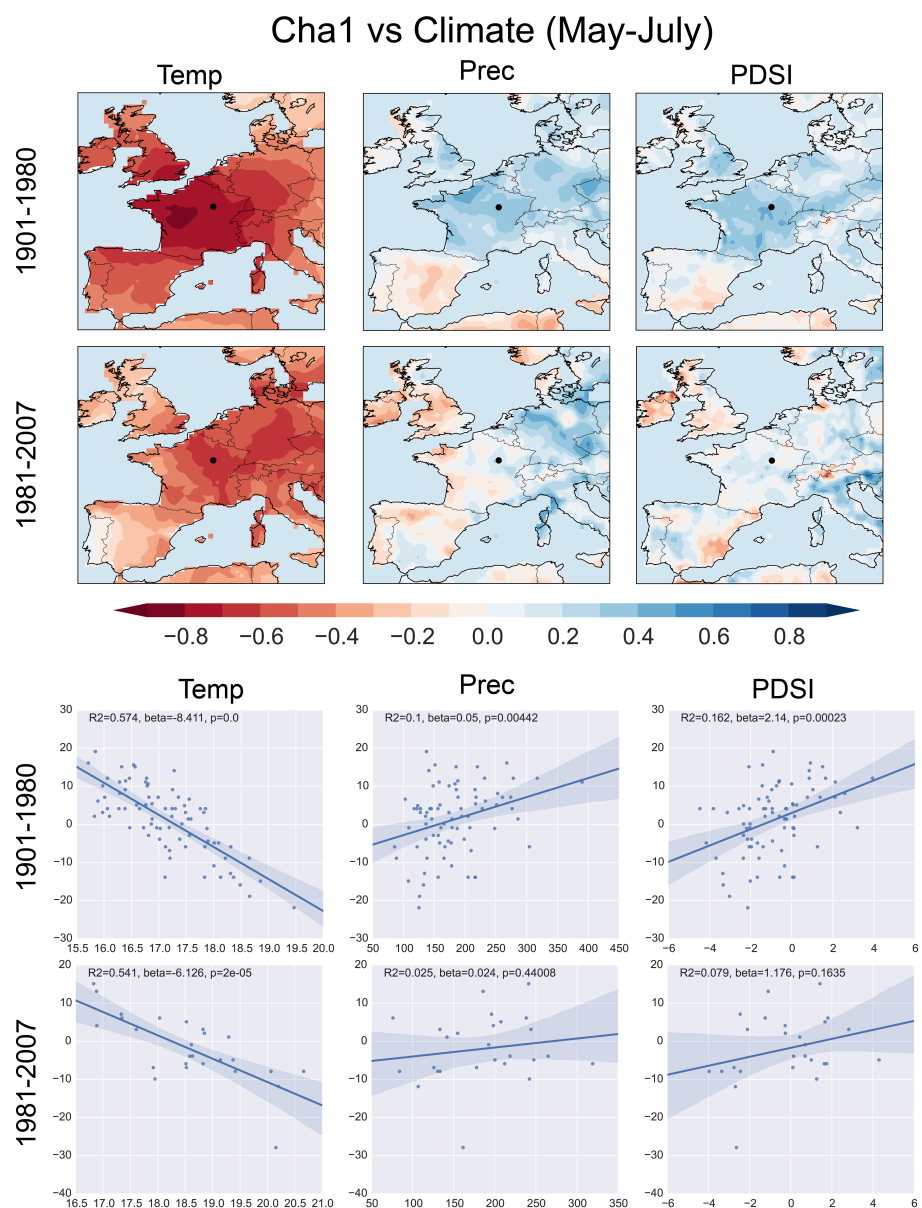
Bor vs Climate (May-July)



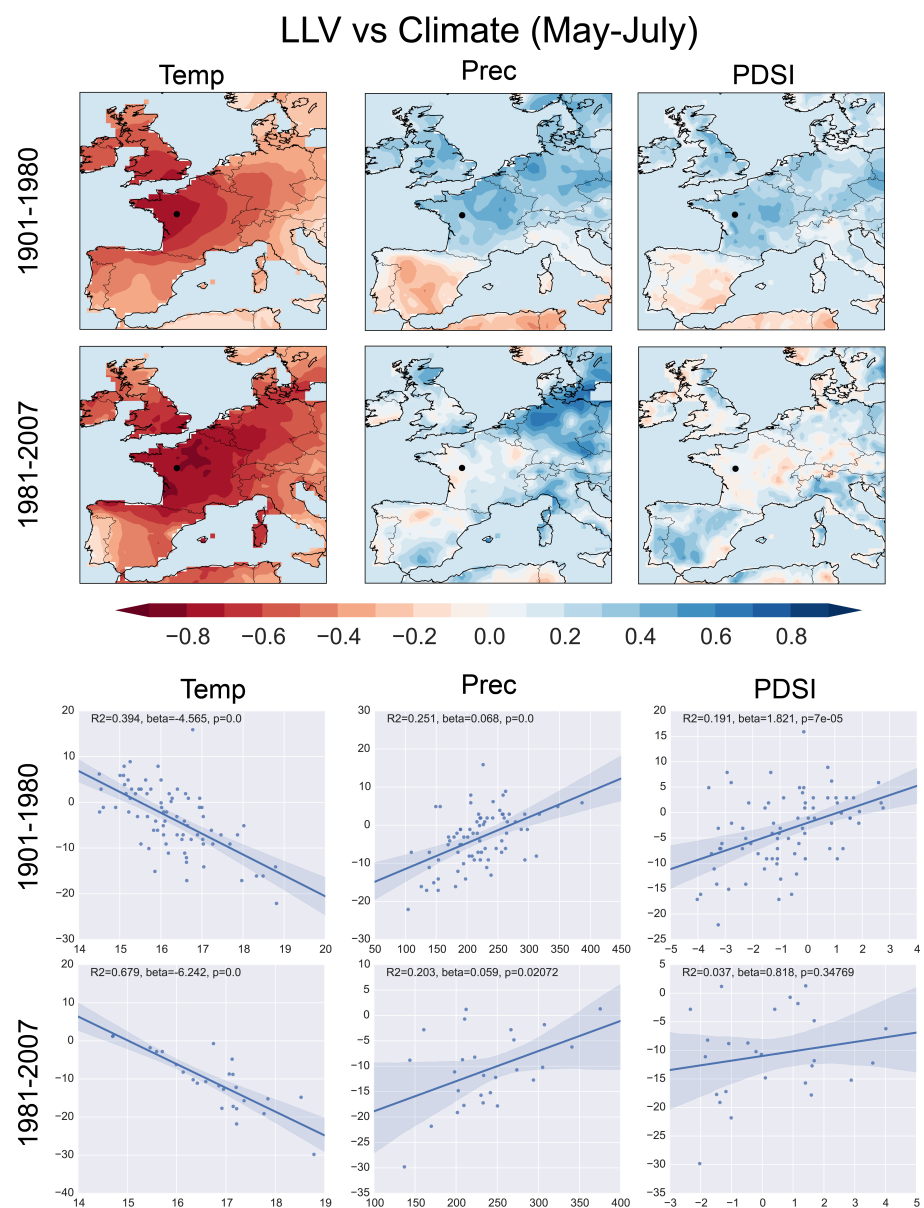
Supplementary Figure 5: Same as Figure 4, but for Bor.



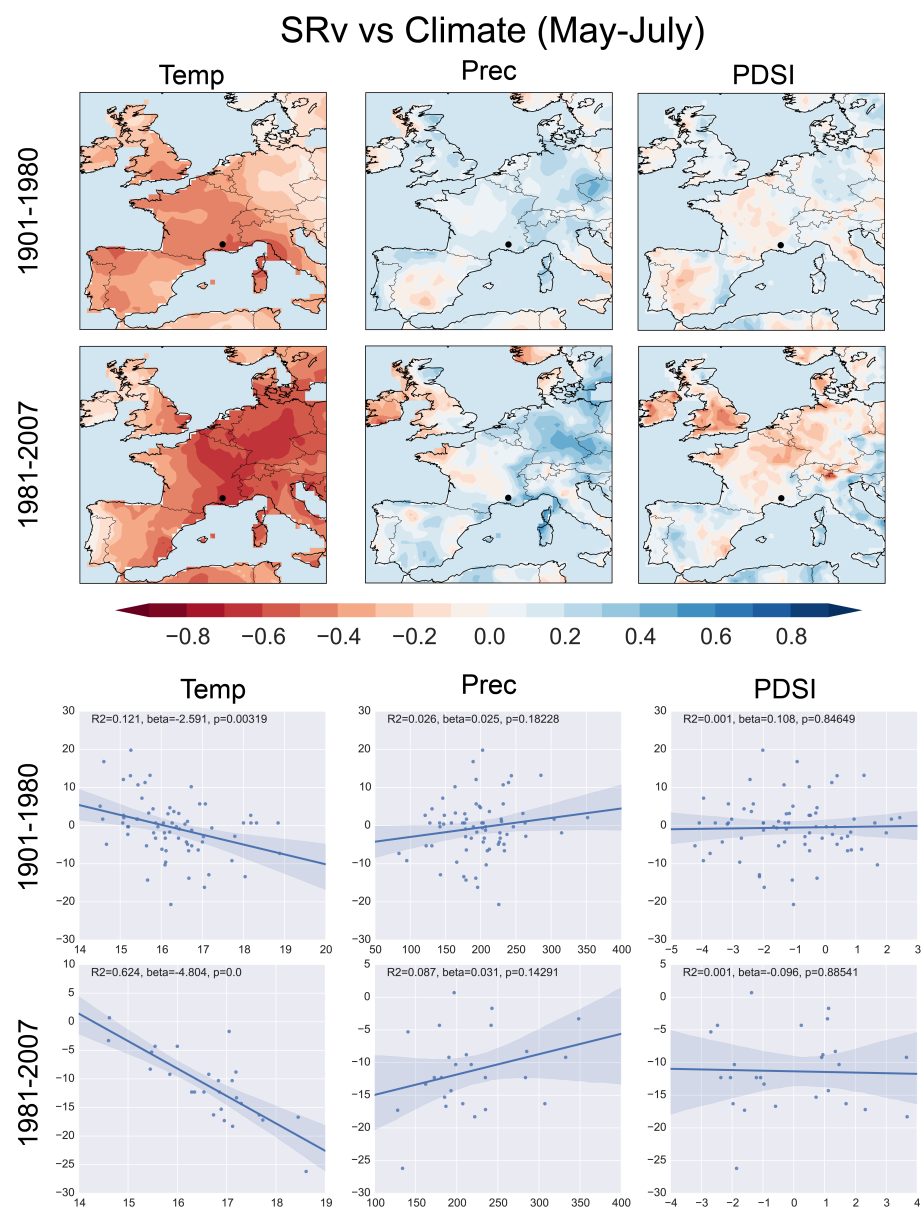
Supplementary Figure 6: Same as Figure 4, but for Bur.



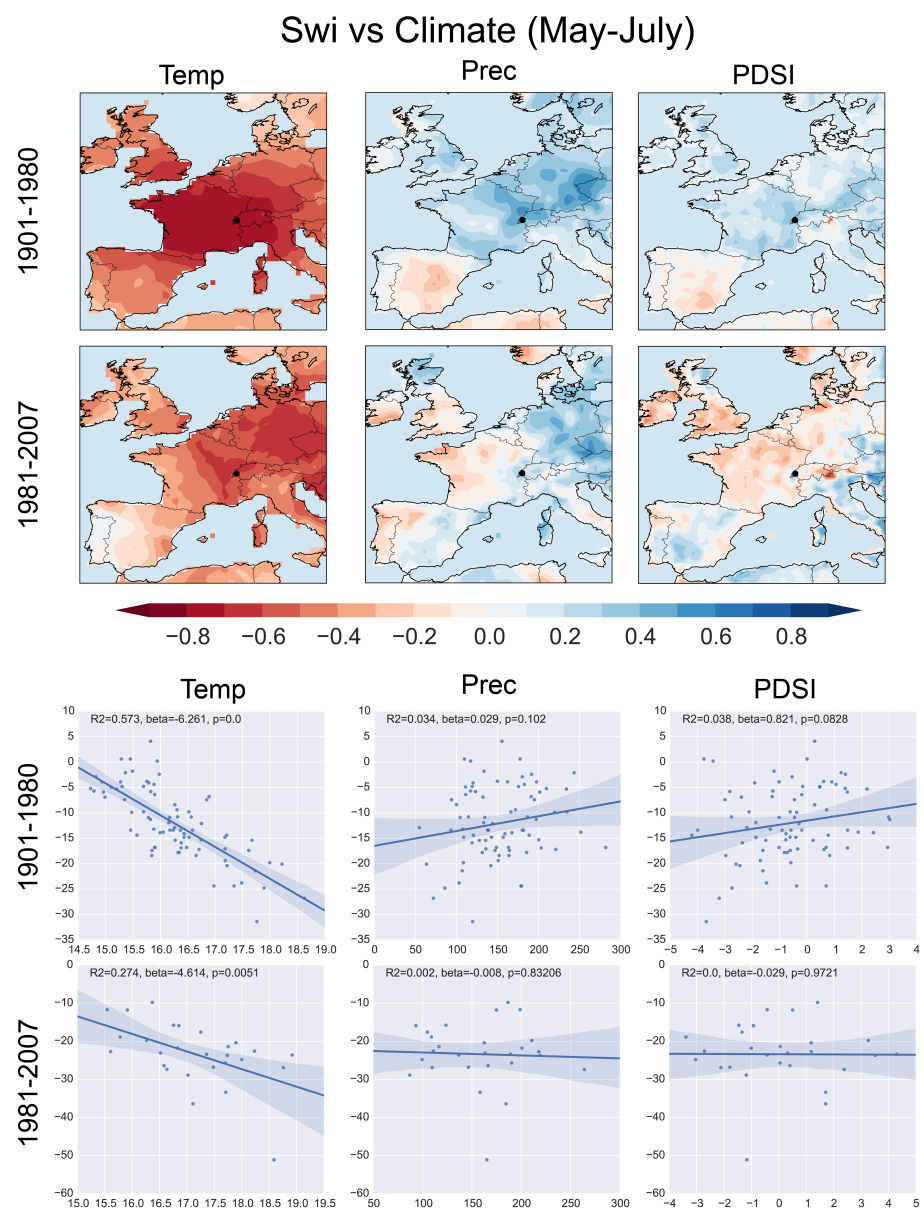
Supplementary Figure 7: Same as Figure 4, but for Cha1.



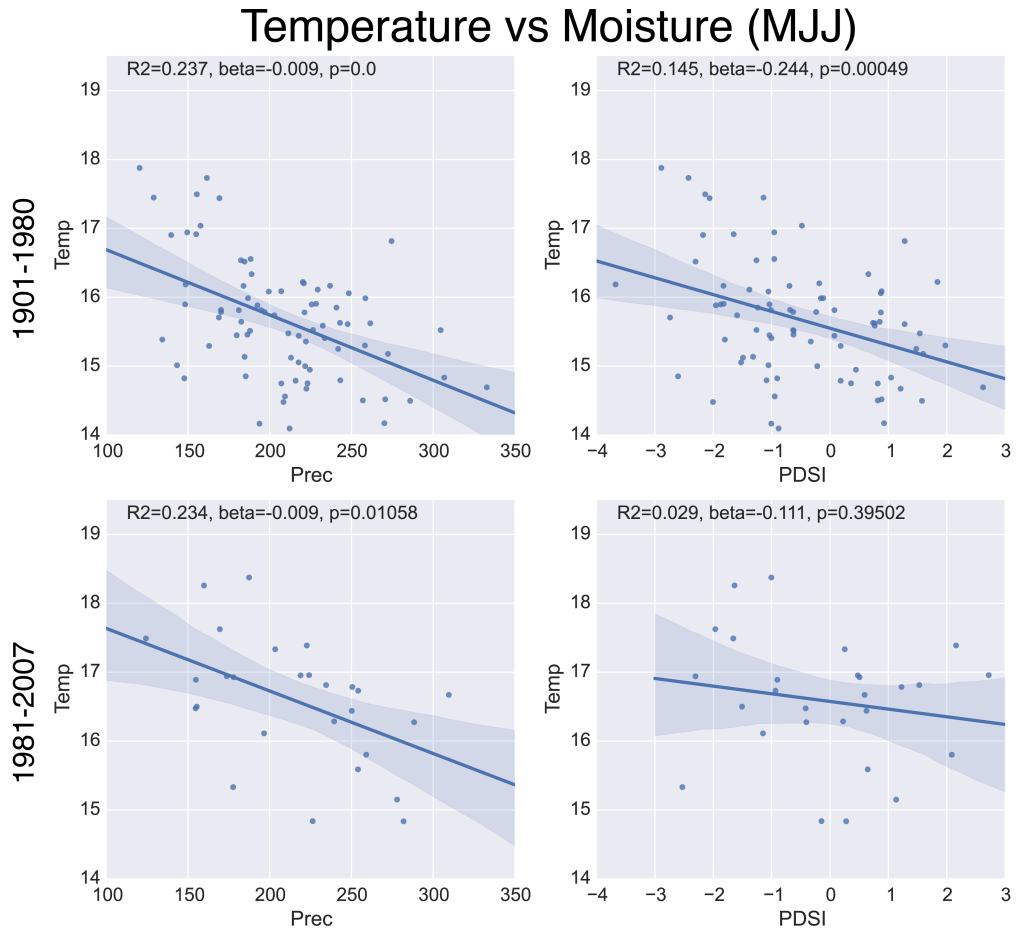
Supplementary Figure 8: Same as Figure 4, but for LLV.



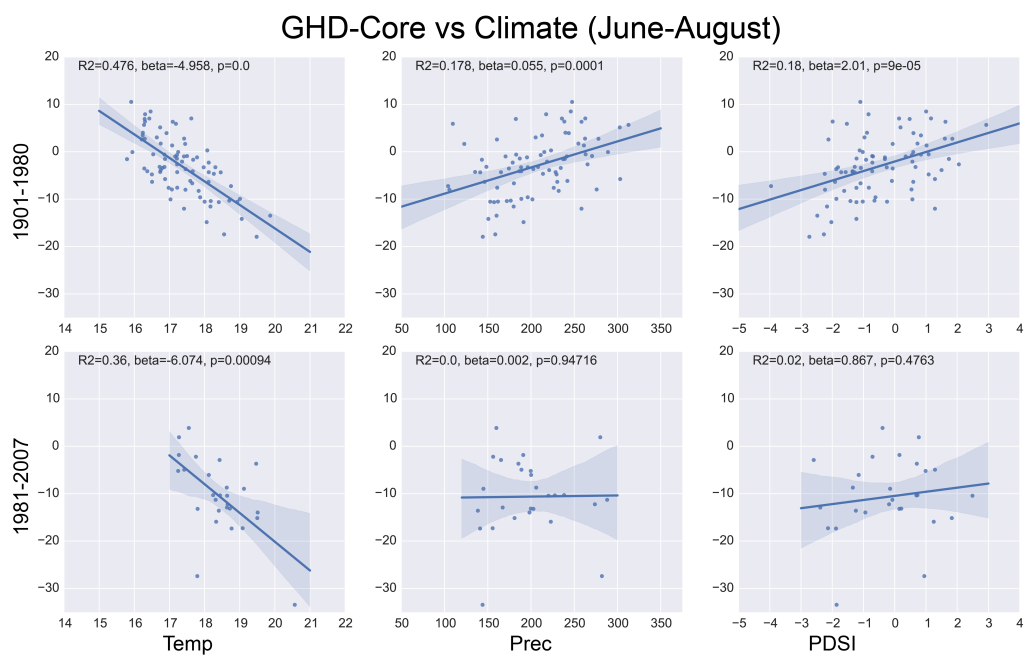
Supplementary Figure 9: Same as Figure 4, but for SRv.



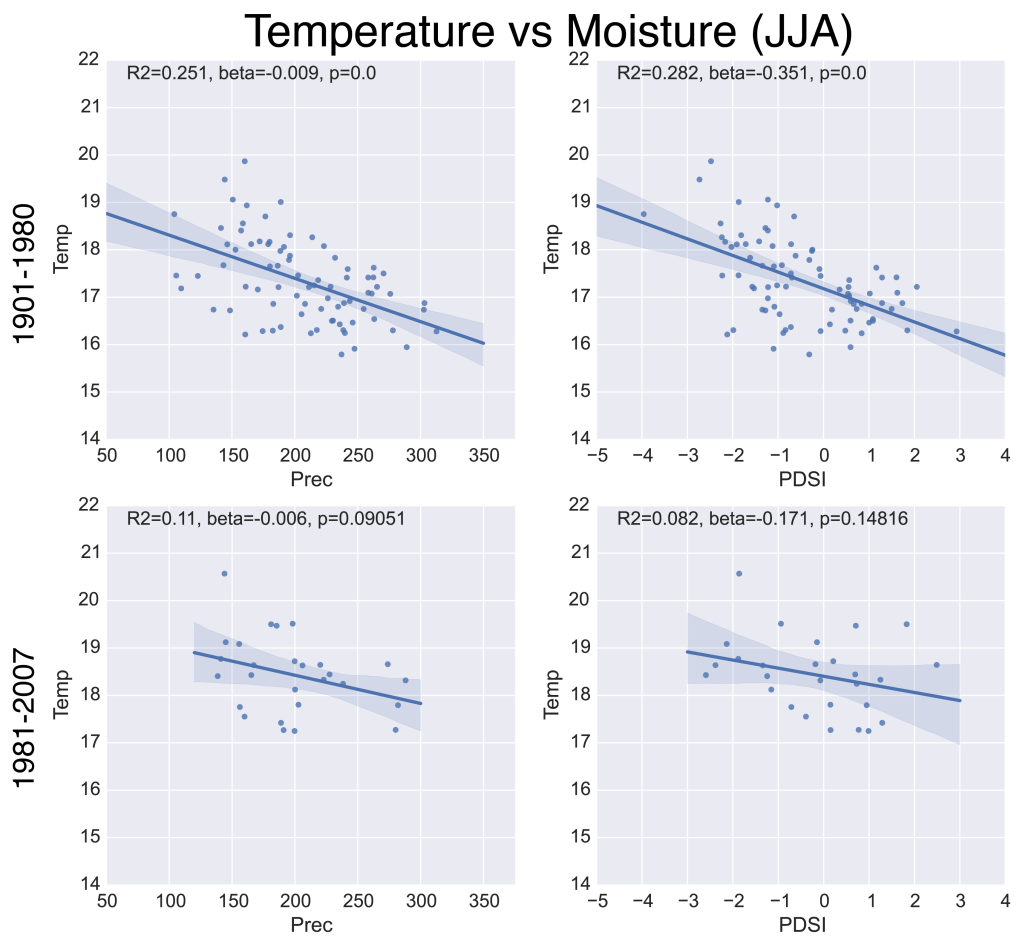
Supplementary Figure 10: Same as Figure 4, but for SWi.



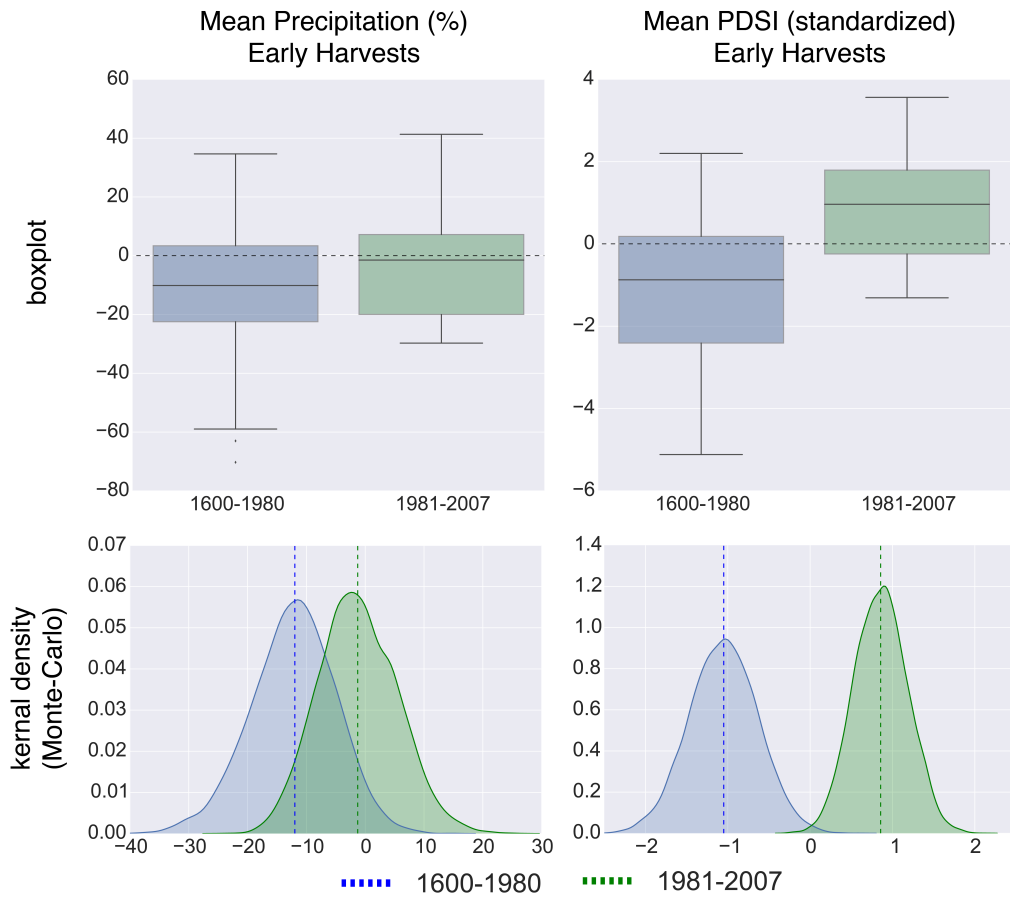
Supplementary Figure 11: Temperature versus moisture (precipitation and PDSI) during May-June-July for the GHD-Core region from the CRU 3.21 climate grids for two periods: 1901–1980 and 1981–2007. Temperature during MJJ has a significant negative relationship with both precipitation and PDSI, indicating the tendency for warmer conditions during drier years. Over the more recent period, the relationship between temperature and PDSI breaks down, but the relationship with precipitation remains largely consistent.



Supplementary Figure 12: Same as Figure 3 from the main manuscript, but for June-July-August (JJA).



Supplementary Figure 13: Same as Supplemental Figure 11, but for June-July-August (JJA) climate. During JJA, the temperature moisture relationship is stronger over this region and, in both precipitation and PDSI, these relationships breakdown in the recent decades (1981–2007).



Supplementary Figure 14: Top row: box plots of pooled precipitation and PDSI anomalies from the climate reconstructions for years with early harvest date anomalies in GHD-Core. Bottom row: kernel density functions of recalculated mean precipitation and PDSI anomalies associated with early harvest dates, based on 10,000 Monte-Carlo resamplings with replacement.